

# Fatigue Life Assessment of Laserbeam Welded Steel Tube-Tube Joints under Constant-amplitude Out-of-phase Combined Axial Loading and Torsion by Integration of Damage Differentials (IDD)

S. Stefanov<sup>1</sup>, J. Wiebesiek<sup>2</sup>, K. Störzel<sup>2</sup>, T. Bruder<sup>2</sup>

<sup>1</sup> Department of Mechanical Engineering and Automation, University LTU of Sofia, Kliment Ohridski Blvd No 10, 1756 Sofia, Bulgaria; Fax: +359 2 8622830  
Email: stefan.stefanov.ltu@abv.bg

<sup>2</sup> Fraunhofer Institute for Structural Durability and System Reliability LBF, Bartningstr. 47, 64289 Darmstadt, Germany; Fax: +49 6151 705-214  
Emails: jens.wiebesiek@lbf.fraunhofer.de, klaus.stoerzel@lbf.fraunhofer.de, thomas.bruder@lbf.fraunhofer.de

**ABSTRACT.** *Laserbeam welded overlapped tube-tube steel joints were tested in LBF. The FE keyhole model was applied for determining the local stresses. S-N lines were obtained under fully reversed sinusoidal pure axial loading, pure torsion, and in-phase (proportionally) combined axial loading and torsion. These S-N lines were used at the input of the present IDD software. Three more experimental S-N lines were also obtained under 90° and 45° out-of-phase combined axial loading and torsion. These lines gave opportunity for new IDD verifications: whether the empirical IDD factors of loading non-proportionality  $f_c$  and  $f_\tau$  obtained and confirmed previously as 2 and 3, as well previous equalities  $N_r = N_c = N_b$  would be confirmed again. The verifications gave a positive answer: the corresponding three IDD computed “out-of-phase” S-N lines agreed fairly well with the experimental ones. The paper contributes to representing, clarifying and advancing the present IDD method that is universally and directly applicable under any multiaxial non-proportional loading.*

## INTRODUCTION

The IDD concept and its present implementation, the present IDD method and software, are generally represented in [1]. Any additional detail can be found on the IDD site: <http://www.freewebs.com/fatigue-life-integral/>. IDD is completely different than all the other known approaches to fatigue life assessment. Damage differentials  $dD$  (little finite damage differences  $\Delta D$ ) are integrated (summed) instead of damages per cycles.

There is a statement in [1] that additional concretized representation of IDD continues in this paper and also in [2, 3]. Besides, experimental IDD verification results are presented here. They relate to the so-called factors of loading non-proportionality  $f_c$

and  $f_\tau$  in Eq. 5 in [1]. As well, the numbers  $N_r$ ,  $N_c$  and  $N_\tau$  [1] are verified in this paper. They limit the zero areas of the so-called damage intensities  $R_r$ ,  $R_c = f_c R_r$  and  $R_\tau = f_\tau R_r$  in the coordinate plane  $\sigma'-\sigma''$  of the principal stresses  $\sigma$  and  $\sigma''$ . Figure 1 illustrates the  $\sigma'-\sigma''$  plane that belongs to the IDD coordinate space  $\sigma'-\sigma''-\Delta\tau$  [1].

What should be primarily represented here in addition to [1] is the so-called lines of equal lives under cyclic (constant-amplitude) proportional loadings. Named also cyclic  $r$ -loadings [1], they have “trajectories”  $(S_r)$  (loading paths) which are radial straight-line segments. As an example, such two radial segments,  $(S_r)_1$  and  $(S_r)_2$ , are shown in Fig. 1. Supposing the lives of the two corresponding cyclic  $r$ -loadings are equal, for example  $10^5$  cycles, then  $(S_r)_1$  and  $(S_r)_2$  are limited by the curved line of equal life labeled with  $10^5$ . All the other possible radial  $(S_r)$  trajectories, with different values of the constant ratio  $k = \sigma''/\sigma$ , will have the same life of  $10^5$  cycles if they reach the same line of equal life  $10^5$ . As another example, a line of equal life  $10^6$  is also illustrated.

The present IDD method composes each line of equal life as consisting of elliptic arcs in a manner which allows covering any experimental or hypothetical line of equal life. Up to 9 input  $S$ - $N$  lines can be entered and they serve for assessment of the fatigue life of any loading having an arbitrary non-radial trajectory  $(S_{xy})$  (Fig. 1). For example, as explained below, the report [4] gives experimental data of IDD input  $S$ - $N$  lines valid for the radial lines (Fig. 1) with the following values of  $k$ : 0,3, 0 and  $-1$ .

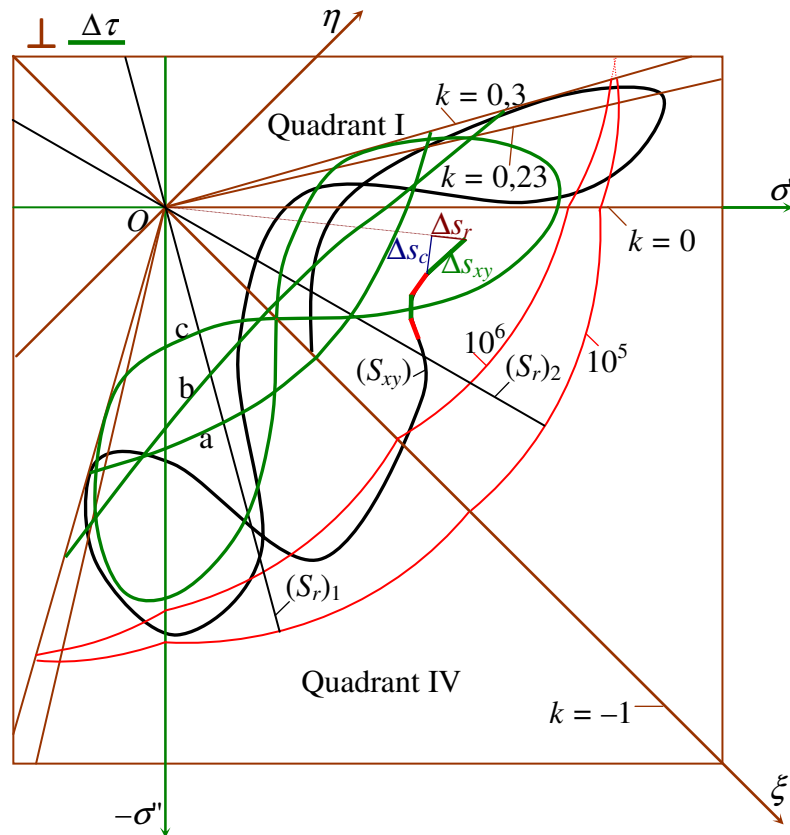


Figure 1. The  $\sigma'-\sigma''$  plane like it appears in graph mode of the IDD software [1]

If  $S$ - $N$  lines, serving for input ones, are obtained, interpreted and drawn correctly, then the corresponding lines of equal lives appear adequately: they do not zigzag too much and do not abruptly concave inwards to the coordinate origin. Each elliptic arc should not turn into a hyperbolic arc concaving inwards. And, the lines of equal lives should not intersect, of course. Figure 1 actually gives an example of two lines of equal lives  $10^5$  and  $10^6$  that are somewhat not correct: they would intersect above  $k = 0,3$ .

In case of incorrect input  $S$ - $N$  lines, the IDD software alarms. If lines of equal lives would intersect, the software refuses to compute. For example, when the running trajectory ( $S_{xy}$ ) in Fig. 1 passes near to the shown possible point of intersection of the lines of equal lives  $10^5$  and  $10^6$ , then the IDD computation will stop.

After the above clarification of the lines of equal lives, it is clear now how the numbers  $N_r$ ,  $N_c$  and  $N_\tau$  limit the zero areas of the damage intensities  $R_r$ ,  $R_c = f_c R_r$  and  $R_\tau = f_\tau R_r$ : the border lines of those zero areas are the lines of equal lives  $N_r$ ,  $N_c$  and  $N_\tau$  [5].

In addition, Fig. 1 shows the current  $\Delta s_{xy}$  element of the running arbitrary trajectory ( $S_{xy}$ ). As represented in [1], the  $\Delta s_{xy}$  element is resolved into  $\Delta s_r$  and  $\Delta s_c$  elements. In case the principal axes rotate, a “perpendicular” element  $\Delta \tau$  also appears (displayed separately by the  $\perp$  symbol of perpendicularity to the  $\sigma$ - $\sigma'$  plane). The elements  $\Delta s_r$ ,  $\Delta s_c$  and  $\Delta \tau$  are components of  $\Delta s$  of the very loading trajectory ( $S$ ): ( $S_{xy}$ ) is a projection of ( $S$ );  $\Delta s$  represents loading differential  $ds$  per which the damage differential  $dD$  (i.e.  $\Delta D$ ) is computed according to Eq. 3 in [1].

For the computation of  $\Delta D$ , the damage intensity  $R_r$  [1] participates at  $\Delta s_r$  together with the factors of non-proportionality  $f_c$  and  $f_\tau$  at  $\Delta s_c$  and  $\Delta \tau$ . As mentioned in [1],  $R_r$  has a heavy mathematical expression. It is derived from the equation of the elliptic arc of the line of equal life onto which the current element  $\Delta s$  falls. The parameters of the input  $S$ - $N$  lines are also involved (see the IDD site for more details). The life of the ( $S$ ) trajectory is computed as number of repetitions until the sum of all the differentials  $\Delta D$  reaches 1: see Eq. 5 in [1].

In [5], three IDD verifications were done. A conclusion was drawn that  $f_c$  and  $f_\tau$  prove to have values 2 and 3 universally under  $90^\circ$ -out-of-phase or different-frequency combined loadings, for steel or cast iron, notched or unnotched specimens, number of cycles to rupture or to a crack. With that, the equalities  $N_c = N_\tau = N_r$  proved to be valid. They do not mean coinciding the zero  $R_r$ ,  $R_c$  and  $R_\tau$  areas: since  $f_\tau > f_c > 1$ , the zero  $R_c$  and  $R_\tau$  areas go more and more inward to the coordinate origin than the zero  $R_r$  area [5]. In this paper, next verifications, based on the experimental data in [4], follow.

## **EXPERIMENTAL DATA [4] UNDER PURE AND IN-PHASE LOADINGS AND THEIR INTERPRETATION FOR COMPOSING INPUT $R_r$ -PROTOTYPES**

### ***The Local Stresses in Laser-beam Welded Tube-tube Steel Joints***

The specimens look as shown in Fig. 2(a). The keyholes, Fig. 2(b), are an FE model of stress concentrators introduced as equivalent to the local stresses in the welded joints. The background of the respective notch stress concepts can be derived from [4].

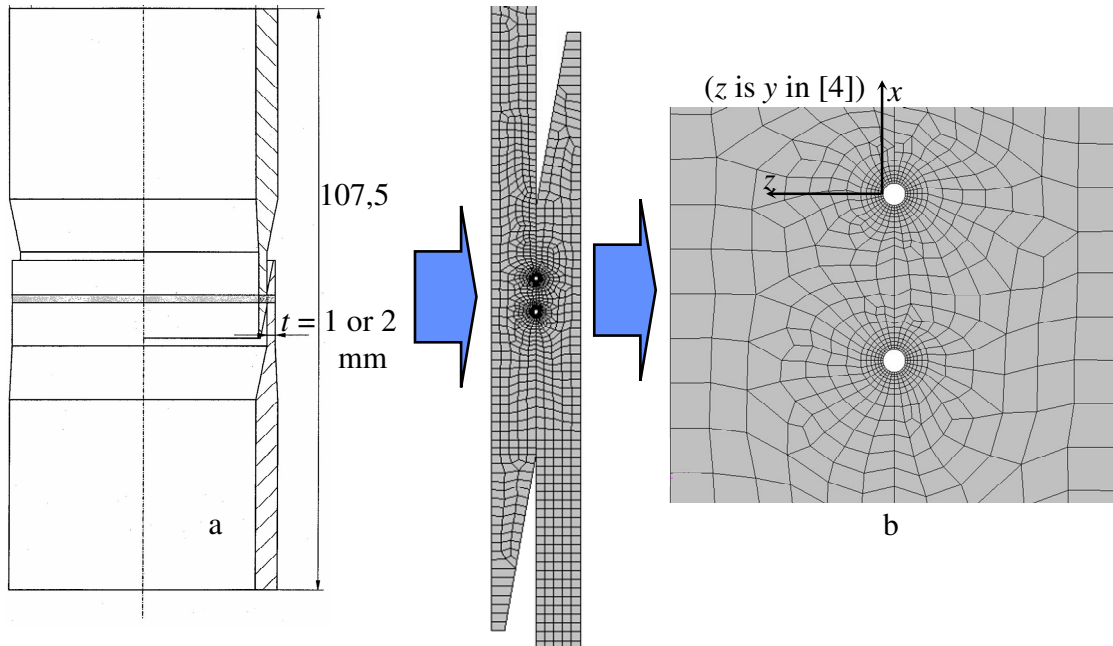


Figure 2. The welded tube-tube specimen (a) and the FE keyhole notch model (b)

The following symbols and relations are available in [4] for maximum local stresses:  $\sigma_{\phi, \max} = 79,7 \text{ MPa/kN}$ ,  $\sigma_{z, \max} = 24,0 \text{ MPa/kN}$  and  $\tau_{\phi z, \max} = -1,41 \text{ MPa/Nm}$ , where kN relates to  $F$  axial force and Nm relates to  $M$  torsional moment. These  $\sigma_{\phi, \max}$ ,  $\sigma_{z, \max}$  and  $\tau_{\phi z, \max}$  do not act on the same critical infinitesimal cuboid (cubic volume). However [4], a series of cuboids round the keyhole, Fig. 2(b), are approximately equally critical and are exerted by  $\sigma_{\phi}$ ,  $\sigma_z$  and  $\tau_{\phi z}$  that are close to  $\sigma_{\phi, \max}$ ,  $\sigma_{z, \max}$  and  $\tau_{\phi z, \max}$ .

Using the symbols  $\sigma_x$ ,  $\sigma_y$  and  $\tau_{xy}$  for IDD [1], the following correspondence applies:  $\sigma_{\phi} \rightarrow \sigma_x$ ,  $\sigma_z \rightarrow \sigma_y$ ,  $-\tau_{\phi z} \rightarrow \tau_{xy}$ . Then, one of the approximately equally critical cuboids can be imagined so, Fig. 2(b): its  $x$  normal line is in the longitudinal (axial) tube's direction, its  $y$  normal line is in the circumferential tube's direction, and its free-of-stress plane (with the  $z$  normal line) belongs to the internal surface of the keyhole. As to the other cuboids, the local  $y$  axis remains in the global tube's circumferential direction but the local axis  $x$  changes its direction from one cuboid to another round the keyhole.

After all, the local stress values in this paper were derived from [4] according to  $\sigma_x/F = 79,7 \text{ MPa/kN}$ ,  $\sigma_y/F = 24,0 \text{ MPa/kN}$ ,  $\tau_{xy}/M = 1,41 \text{ MPa/Nm}$ . The loadings done [4] are:

- pure axial ( $\sigma_y/\sigma_x = 0,3$ ,  $\sigma'/\sigma_x = 1,0$ ,  $k = \sigma''/\sigma' = 0,3$  (which is the Poisson ratio);
- in-phase combined (proportional),  $M/F = 12 \text{ Nm/kN}$  ( $\tau_{xy}/\sigma_x \approx 0,21$ ,  $\sigma_y/\sigma_x = 0,3$ ,  $\sigma'/\sigma_x = 1,06$ ,  $k = \sigma''/\sigma' \approx 0,23$ );
- in-phase combined (proportional),  $M/F = 28 \text{ Nm/kN}$  ( $\tau_{xy}/\sigma_x \approx 0,5$ ,  $\sigma_y/\sigma_x = 0,3$ ,  $\sigma'/\sigma_x = 1,26$ ,  $k = \sigma''/\sigma' \approx 0,035$  (what means nearly uniaxial stressing);
- pure torsion ( $\sigma' = \tau_{xy}$ ,  $k = \sigma''/\sigma' = -1$ ).

### **The Experimental Data and Composing the Input $R_r$ -prototypes**

The experimental points [4] were transferred here into Fig. 3. Their scatter looks great.

However, it is normal for such complicatedly notched specimens.

For IDD, the  $\bullet$  points (only  $F$ ,  $k = 0,3$ ) and the  $\circ$  points ( $M/F = 12$  kN/m,  $k \approx 0,23$ ) practically belong to one and the same  $S-N$  line as an  $\sigma'_a-N$  line. Indeed, the corresponding above ratios  $\sigma'/\sigma_x$  differ insignificantly: 1,0 and 1,06. That is why the points  $\bullet$  and  $\circ$  were united. The corresponding single  $S-N$  line can be considered either valid for an intermediate  $k$  radial line or for any of the two radial lines with  $k = 0,3$  and  $k = 0,23$  (see Fig. 1), without any significant influence;  $k = 0,3$  was accepted.

Moreover, if trying to draw two different  $S-N$  lines separately among the points  $\bullet$  and  $\circ$ , they will be in some conflict ( $\circ$  must have been all to the left from  $\bullet$ ). Such two different  $S-N$  lines will make the lines of equal lives abnormal and trending to intersect: the IDD software will alarm for impossibility to compute.

Among the three groups of points in Fig. 3, smoothly curved  $S-N$  lines were drawn [4]. They correspond to the IDD equation  $(s^m - s_r^m)N = A = \text{constant} = s_r^m N_r$  [1]. As known from [1], such an  $S-N$  line is reproduced by IDD from an  $R_r$ -prototype as a straight line with the equation  $s^m N = A = s_r^m N_r$ . Each curved  $S-N$  line should truthfully appear among the scattered points what was provided as follows.

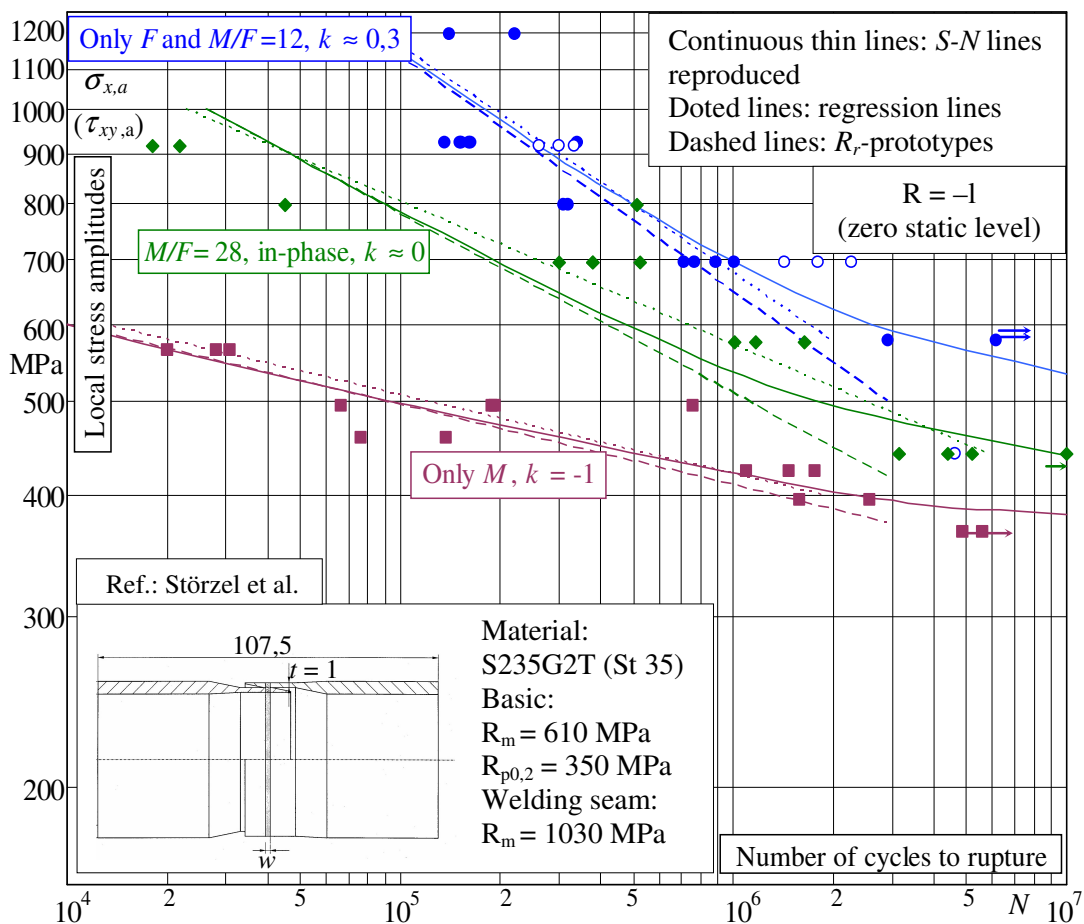


Figure 3. Experimental points, curved  $S-N$  lines reproduced and straight  $R_r$ -prototypes

First, the three regression lines (Fig. 3) were obtained according to the least squares method after excluding the run-outs. Their equations, for  $k \approx 0,3$ ,  $k \approx 0$  and  $k = -1$ , are  $\sigma_{x,a}^{4,25}N = 1,058.10^{18}$ ,  $\sigma_{x,a}^{6,736}N = 3,694.10^{24}$  and  $\tau_{x,a}^{12,27}N = 1,546.10^{38}$ . In next approximation, each reproduced  $S-N$  line was obtained taking into account the run-outs that make it curve. It is to note that all the  $R_r$ -prototypes are assumed to have the same  $N_r$  in  $s_r^m N_r = A$  so that the line of equal life  $N_r$  should serve as a borderline of the zero  $R_r$  area. These requirements lead to a series of calculation trials for good agreement and finding the parameters of both the reproduced input  $S-N$  lines and the  $R_r$ -prototypes.

After doing these calculation trials,  $N_r$  was found out as  $2,9.10^6$ . The three  $R_r$ -prototype equations proved to be  $\sigma_{x,a}^{4,1}N = 500^{4,1}2,9.10^6$ ,  $\sigma_{x,a}^{5,4}N = 418^{5,4}2,9.10^6$  and  $\tau_{x,a}^{12}N = 374^{12}2,9.10^6$ . Correspondingly, the three  $S-N$  lines reproduced have the equations  $(\sigma_{x,a}^{4,1} - 500^{4,1})N = 500^{4,1}2,9.10^6$ ,  $(\sigma_{x,a}^{5,4} - 418^{5,4})N = 418^{5,4}2,9.10^6$  and  $(\tau_{x,a}^{12} - 374^{12})N = 374^{12}2,9.10^6$ .

After having the equations of the  $R_r$ -prototypes, an L-file [1], named L1, was composed by the *EllipseT* program [1]. This file, as well the next so-called C-files [1] can be reproduced by everyone following the instructions on the IDD site. Besides, all the files relating to this paper will be placed on the IDD site after ICMFF9 is held.

## EXPERIMENTAL AND COMPUTED LIVES UNDER OUT-OF-PHASE COMBINED LOADINGS

**90°-out-of-phase,  $M/F = 28 \text{ Nm/kN}$  ( $\tau_{xy,a}/\sigma_{x,a} \approx 0,5$ )**

In Fig. 4, the experimental points [4] are shown. Among them, the 90°-out-of-phase  $S-N$

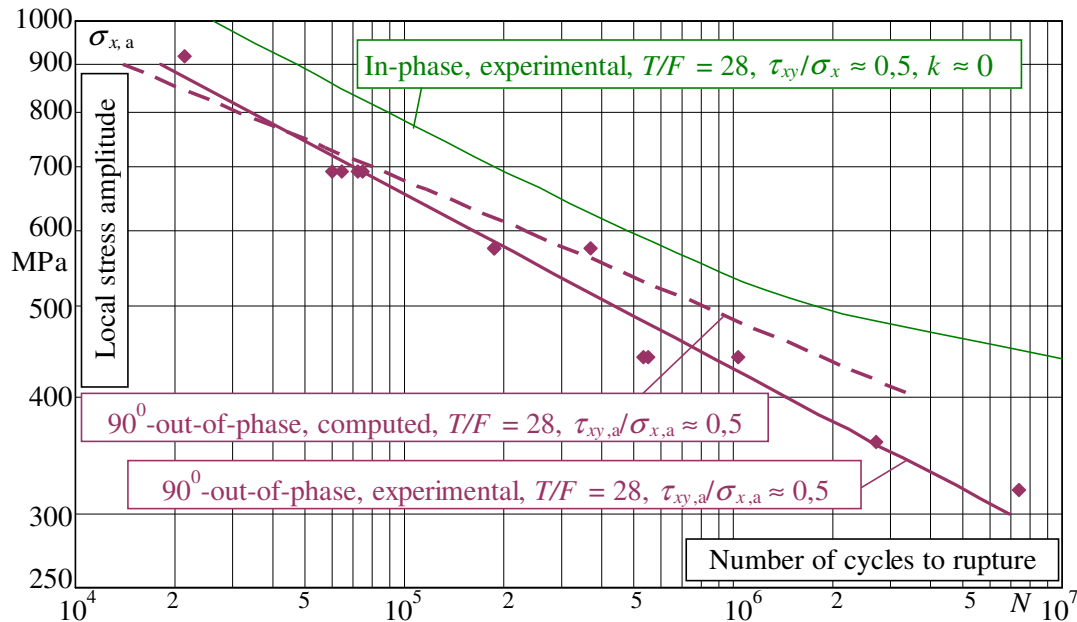


Figure 4. The experimental and computed  $S-N$  lines under the 90°-out-of-phase combined loading with  $M/F = 28 \text{ Nm/kN}$



line was drawn as a regression line (it passes through a point with coordinates 900 and 18077 and has a slope  $m = 5,41$ ). It is shifted to the left from the in-phase  $S-N$  line i.e. the effect of a life decrease due to the  $90^0$ -out-of-phase angle is available.

Computed lives were obtained at loading levels 900, 600 and 400 MPa (Fig. 4). Corresponding C-files named C900-1, C600-1 and C400-1 were composed by the *EllipseT* program. The IDD factors of non-proportionality  $f_c = 2$  and  $f_\tau = 3$ , as well as  $N_c = N_\tau = N_r (= 2,9 \cdot 10^6$  in this verification) were again set in L1 like in the previous verifications [5]. The three computed lives proved to be 13820, 231800 and 3556000 against the experimental 18077, 161860 and 1449276 from the regression line.

**$90^0$ -out-of-phase,  $M/F = 12 \text{ Nm/kN}$  ( $\tau_{xy,a}/\sigma_{x,a} \approx 0,21$ )**

In Fig. 5, like above, the experimental  $90^0$ -out-of-phase  $S-N$  line was drawn as a regression line among the experimental points [4] (it passes through a point with coordinates 700 and 386478 and has a slope  $m = 6,25$ ). As already expected, it is shifted again to the left from the in-phase  $S-N$  line. Loading levels were selected to be 700, 600 and 500 MPa for computation of lives. Corresponding C-files named C700-2, C600-2 and C500-2 were composed. Again L1 was involved.

The three computed lives turned out 347700, 728400 and 1909000 against the experimental 386480, 1012300 and 3161653. Now the computed lives deviate from the experimental lives to the safety side, unlike above.

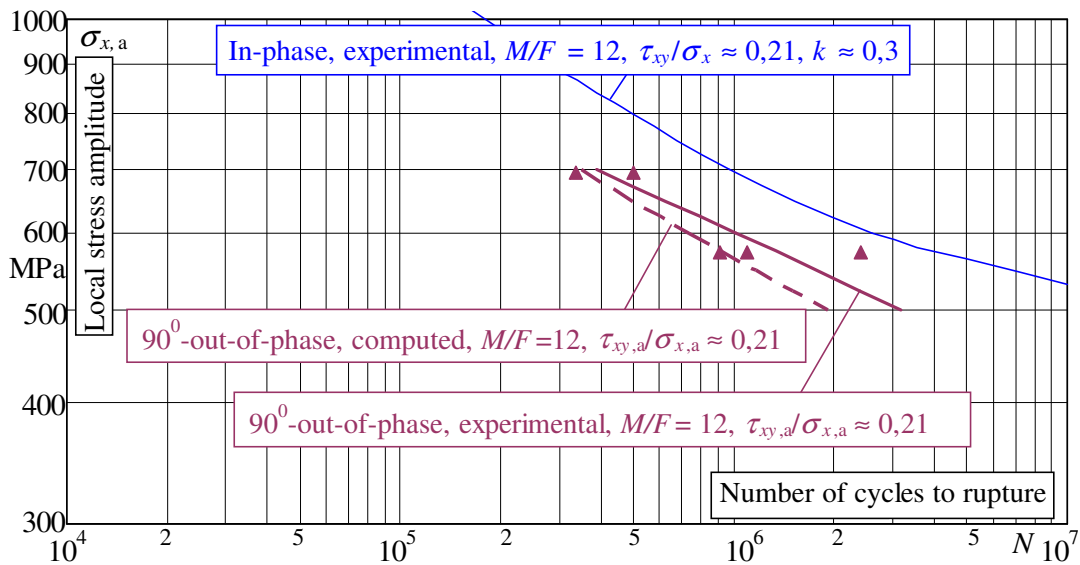


Figure 5. The experimental and computed  $S-N$  lines under the  $90^0$ -out-of-phase combined loading with  $M/F = 12 \text{ Nm/kN}$

**$45^0$ -out-of-phase,  $M/F = 28 \text{ Nm/kN}$  ( $\tau_{xy,a}/\sigma_{x,a} \approx 0,5$ )**

In Fig. 6, the regression line passes through a point with coordinates 700 and 120198, and has a slope  $m = 5,09$ . Lives were computed at loading levels 700, 550 and 440 MPa. The C-files are named C700-3, C550-3 and C440-3. The three computed lives turned out 92030, 367100 and 1473000 against experimental 120198, 409989 and 1275945.

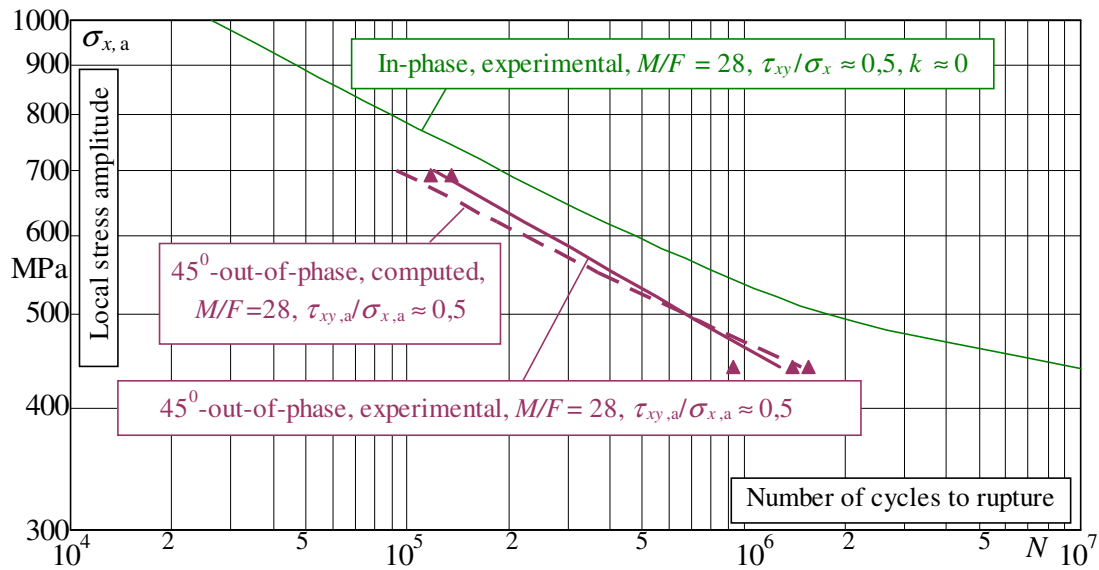


Figure 6. The experimental and computed  $S-N$  lines under the  $45^0$ -out-of-phase combined loading ( $M/F = 28$  Nm/kN)

By the way, an  $(S_{xy})$  trajectory “ $45^0$ -out-of-phase/  $M/F = 28$ ” looks like “c” in Fig. 1 (“8” form), whereas the  $(S_{xy})$  trajectories “ $90^0$ -out-of-phase/  $M/F = 28$ ” and “ $90^0$ -out-of-phase/  $M/F = 12$ ” look like “b” and “a” (for similar cases see [5] or/and the IDD site).

## CONCLUSION

The nine values of the ratio  $N_{cmp}/N_{exp}$  of the computed  $N_{cmp}$  and experimental  $N_{exp}$  lives have an average of 1,03 (between a minimum of 0,47 and a maximum of 2,45) and a standard deviation of 0,45. These data, as well as the look of the Figs 4 – 6, testify for good agreement between  $N_{cmp}$  and  $N_{exp}$ . That is, the equations  $f_c = 2$ ,  $f_\tau = 3$  and  $N_c = N_\tau = N_r$ , confirmed in [5], prove valid again. Thus, they, unrevised, will be used next [2, 3].

## REFERENCES

1. Stefanov, S.H. (2010). In: *Proc. ICMFF9*, In Press.
2. Sonsino, C.M., Stefanov, S.H. (2010). In: *Proc. ICMFF9*, In Press.
3. Stoychev, B.I, Stefanov, S.H. (2010). In: *Proc. ICMFF9*, In Press.
4. Störzel, K., Wiebesiek, J., Bruder, T., Hanselka, H. (2008) *Betriebsfeste Bemessung von mehrachsigt belasteten Laserstrahlschweisverbindungen aus Stahlfeinblechen des Karosseriebaus/ Bericht Nr. FB-235*, Fraunhofer-Institut für Betriebsfestigkeit LBF, Darmstadt, Germany.
5. Stefanov, S.H., Hanselka, H., Sonsino, C.M. (2009) *Application of IDD (Integration of Damage Differentials) for Fatigue Life Assessment/ LBF Report No. FB-236*, Fraunhofer Institute LBF, Darmstadt, Germany.